DTU Library

Dual polarization nonlinear Fourier transform-based optical communication system: supplementary material

Gaiarin, Simone; Perego, A. M.; Porto da Silva, Edson; Da Ros, Francesco; Zibar, Darko

Published in:
Optica

Publication date:
2019

Document Version
Publisher's PDF, also known as Version of record

Link back to DTU Orbit

optica

Dual polarization nonlinear Fourier transform-based optical communication system: supplementary material

S. Gaiarin[1,*], A. M. Perego[2,*], E. P. da Silva[1], F. Da Ros[1], and D. Zibar[1]

[1]*DTU Fotonik, Technical University of Denmark, Lyngby, 2800 Denmark*
[2]*Aston Institute of Photonic Technologies, Aston University, Aston Express Way, Birmingham, B4 7ET UK*
[*]*Corresponding authors: simga@fotonik.dtu.dk, peregoa@aston.ac.uk*

This document provides supplementary information to "Dual polarization nonlinear transform-based optical communication system," **https://doi.org/10.1364/optica.5.000263**. We present the mathematical derivation of the forward-backward trapezoidal algorithm for the Manakov system, which allows the efficient computation of the scattering data from the time domain dual polarization signal. We furthermore describe the optimization procedure followed in order to choose the scattering coefficients constellations for the transmission focusing on the approach we applied to minimize the peak-to-average power ratio of the transmitted waveform. Finally we present a brief analysis of the noise affecting the eigenvalue and the scattering coefficients.

1. NUMERICAL METHODS

We report here the derivation of an algorithm based on the so-called trapezoidal discretization method that allows computing with small numerical errors the scattering coefficients from time domain signals in the Manakov system.

It has been explained in the main paper that in order to compute the scattering coefficients $a(\lambda)$ and $b_{1,2}(\lambda)$, it is required to propagate the Jost solution $\phi^N(t, \lambda)$ from $t = -\infty$ to $t = +\infty$ by integrating Eq. (5b). Among the many integration methods available, from the simple Newton integration to the more complex Runge-Kutta method, it has been shown in [?] that the trapezoidal integration is one of the algorithms that provides the best results in term of numerical precision in the nonlinear Fourier transform (NFT) context for the single polarization case (nonlinear Schrödinger equation (NLSE)). Moreover, in the same work, it was proposed an improvement to the trapezoidal integration, called the forward-backward method, that allows to increase the precision in computing the discrete scattering coefficients for the complex discrete eigenvalues. In section A, we extend the proposed algorithm to the dual polarization Manakov-Zakharov-Shabat spectral problem (MZSP). In section B the concept of trapezoidal integration will be reviewed and following the same procedure used in [?] we will derive the algorithm required to compute the direct NFT for the dual polarization case.

A. The trapezoidal discretization method

The initial value problem (IVP)

$$\frac{d\psi(t)}{dt} = \mathbf{A}(t)\psi(t), \quad \psi(T_1) = \psi_0 \qquad \text{(S1)}$$

where $\mathbf{A}(t)$ is a $n \times n$ matrix, admits the closed solution

$$\psi(t) = \exp\left(\int_{T_1}^t \mathbf{A}(\tau)d\tau\right)\psi_0 \qquad \text{(S2)}$$

if the matrix commutes with itself $\mathbf{A}(t_i)\mathbf{A}(t_j) = \mathbf{A}(t_j)\mathbf{A}(t_i)$ for any given t_i, t_j [?]. The integral in Eq. (S2) can be computed using the trapezoidal integration method. In this way, starting from the initial solution ψ_0 at $t_0 = T_1$, it is possible to numerically compute the solution at an instant $t_N = T_2$ by discretizing the time axis in N sections of length $h = (T_2 - T_1)/N$ and computing the integral as

$$\psi(T_2) = \exp\left\{h\sum_{n=0}^N \frac{1}{2}\left[\mathbf{A}(t_n) + \mathbf{A}(t_{n+1})\right]\right\}\psi_0 + R_e$$

$$= \left[\prod_{n=0}^N e^{\frac{h}{2}\mathbf{A}(t_n)}e^{\frac{h}{2}\mathbf{A}(t_{n+1})}\right]\psi_0 + R_e$$

$$= e^{\frac{h}{2}\mathbf{A}(t_0)}\left[\prod_{n=1}^{N-1} e^{h\mathbf{A}(t_n)}\right]e^{\frac{h}{2}\mathbf{A}(t_N)}\psi_0 + R_e \qquad \text{(S3)}$$

being R_e the truncation error.

If $\tilde{\mathbf{A}}(t)$ is a piecewise constant matrix defined as

$$\tilde{\mathbf{A}}(t) = \begin{cases} \mathbf{A}(t_1) & T_1 \leq t < T_1 + h/2 \\ \mathbf{A}(t_n) & T_1 + nh - h/2 \leq t < T_1 + nh + h/2 \\ \mathbf{A}(t_2) & T_2 - h/2 \leq t < T_2 \end{cases} \quad \text{(S4)}$$

than the solution $\psi(T_2)$ for $\mathbf{A} = \tilde{\mathbf{A}}(t)$ computed using the trapezoidal integration rule is the exact solution of Eq. (S2) ($R_e = 0$). If $\mathbf{A}(t)$ does not satisfy the commutation property, then we can approximate it with $\tilde{\mathbf{A}}$ and compute the approximate solution with the trapezoidal rule.

As explained in the main paper, in order to compute the direct NFT it is necessary to solve the IVP for the time evolution equation of the MZSP

$$\frac{\partial v(t)}{\partial t} = \mathbf{P}(t)v(t)$$
$$= \begin{pmatrix} -i\lambda & q_1(t) & q_2(t) \\ -q_1^*(t) & i\lambda & 0 \\ -q_2^*(t) & 0 & i\lambda \end{pmatrix} v(t) \quad \text{(S5)}$$

with initial condition $v(-\infty) = \phi^N(t,\lambda)|_{t=-\infty}$. Given the assumption that the signal must have a finite and symmetric support, so that $|q_j(t)| = 0, j = 1,2$ for $t \notin [-T_0, T_0]$, we want to find the value of $v(t)$ at $t = T_0$ in order to compute the scattering coefficients $a(\lambda)$ and $b_{1,2}(\lambda)$.

To do this, it is first convenient to perform a change of variable and define the new vector ψ as follow

$$\psi = \begin{pmatrix} \psi_1 \\ \psi_2 \\ \psi_3 \end{pmatrix} = \begin{pmatrix} v_1 e^{i\lambda t} \\ v_2 e^{-i\lambda t} \\ v_3 e^{-i\lambda t} \end{pmatrix} \quad \text{(S6)}$$

The transformed IVP becomes

$$\frac{\partial \psi(t)}{\partial t} = \mathbf{F}(t)\psi(t)$$
$$= \begin{pmatrix} 0 & q_1(t)e^{2i\lambda t} & q_2(t)e^{2i\lambda t} \\ -q_1(t)^* e^{-2i\lambda t} & 0 & 0 \\ -q_2(t)^* e^{-2i\lambda t} & 0 & 0 \end{pmatrix} \psi(t) \quad \text{(S7)}$$

with initial condition ψ_0, the transformed Jost solution reads $\psi^N(-T_0) = (1,0,0)^T$. The scattering coefficients can be computed from the transformed vector as

$$a(\lambda) = \lim_{t \to \infty} \psi_1^N(t) \quad \text{(S8a)}$$
$$b_1(\lambda) = \lim_{t \to \infty} \psi_2^N(t) \quad \text{(S8b)}$$
$$b_2(\lambda) = \lim_{t \to \infty} \psi_3^N(t). \quad \text{(S8c)}$$

Given that $\mathbf{F}(t)$ does not commute with itself for two arbitrary time instants, it is not possible to express the solution of Eq. (S7) as a matrix exponential in the form of Eq. (S2). Nonetheless, as explained before, we can consider the discretized version of $\mathbf{F}(t)$, defined as in Eq. (S4) with $T_1 = -T_0$ and $T_2 = T_0$

$$\tilde{\mathbf{F}}(t_n, \lambda) = \begin{pmatrix} 0 & q_1 e^{2i\lambda t_n} & q_2 e^{2i\lambda t_n} \\ -q_1^* e^{-2i\lambda t_n} & 0 & 0 \\ -q_2^* e^{-2i\lambda t_n} & 0 & 0 \end{pmatrix}. \quad \text{(S9)}$$

Performing the eigenvalue decomposition and computing the exponential of this matrix we obtain

$$\mathbf{G}_n = e^{\mathbf{F}(t_n, \lambda)h} \quad \text{(S10)}$$
$$= \begin{pmatrix} \cos(ph) & \frac{q_1 e^{2i\lambda t_n} \sin(ph)}{p} & \frac{q_2 e^{2i\lambda t_n} \sin(ph)}{p} \\ -\frac{q_1^* e^{-2i\lambda t_n} \sin(ph)}{p} & \frac{|q_2|^2 + |q_1|^2 \cos(ph)}{p^2} & \frac{q_2 q_1^* (\cos(ph)-1)}{p^2} \\ -\frac{q_2^* e^{-2i\lambda t_n} \sin(ph)}{p} & \frac{q_1 q_2^* (\cos(ph)-1)}{p^2} & \frac{|q_1|^2 + |q_2|^2 \cos(ph)}{p^2} \end{pmatrix}$$

with $p = \sqrt{|q_1|^2 + |q_2|^2}$. It should be noted that $\mathbf{G}_n$ reduces to the NLSE case [?] if either q_1 or q_2 goes to zero. Now, one can calculate the $a(\lambda)$ and $b_{1,2}(\lambda)$ coefficients starting from $\psi^N(-T_0)$ and using the rule in Eq. (S3) as follows

$$\begin{pmatrix} a_N(\lambda) \\ b_{1N}(\lambda) \\ b_{2N}(\lambda) \end{pmatrix} = \mathbf{G}_N^{\frac{1}{2}} \mathbf{G}_{N-1} ... \mathbf{G}_2 \mathbf{G}_1 \mathbf{G}_0^{\frac{1}{2}} \begin{pmatrix} 1 \\ 0 \\ 0 \end{pmatrix}. \quad \text{(S11)}$$

B. Forward-backward method

As stated in [?], the forward-backward method can increase the numerical precision in the computations of $b_{1,2}(\lambda_i)$ for the complex discrete eigenvalues λ_i. Indeed, the coefficients $b_{1,2}(\lambda_i)$ are related to the second and third component of ψ which at every integration step changes proportionally to $qe^{2i\lambda_i t}$, as it can be seen from Eq. (S7). Being the imaginary part of the eigenvalue strictly positive, when $T_0 \gg 1$, small errors in the estimation of λ_i can lead to big integration errors due to the real part of the exponential term.

If λ_i is a discrete eigenvalue, by definition $a(\lambda_i) = 0$, so that the projection in Eq. (7a) of the main paper reduces to

$$\phi^N(t, \lambda_i) = \phi^P(t, \lambda_i)b(\lambda_i) \quad \text{(S12)}$$

Since $b_{1,2}(\lambda_i)$ are time-invariant they can be computed at any instant of time by solving the system of equations above. It is convenient to compute thrm at a time instant where the numerical error is small, for instance at $t_m = 0$.

To do this we can propagate forward the Jost solution $\phi^N(t, \lambda_i)$ from $-T_0$ to t_m, and the Jost solution $\phi^P(t, \lambda_i)$ backward from T_0 to t_m in the following way

$$w(t_m) = \mathbf{L}_N \begin{pmatrix} 1 \\ 0 \\ 0 \end{pmatrix} \quad \text{(S13a)}$$

$$u(t_m) = \mathbf{R}_N^{-1} \begin{pmatrix} 0 & 0 \\ 1 & 0 \\ 0 & 1 \end{pmatrix} \quad \text{(S13b)}$$

being $\mathbf{R}_N = \mathbf{G}_N^{\frac{1}{2}} \mathbf{G}_{N-1} ... \mathbf{G}_{m+1}$ and $\mathbf{L}_N = \mathbf{G}_m ... \mathbf{G}_2 \mathbf{G}_1 \mathbf{G}_0^{\frac{1}{2}}$ with $m = \lfloor cN \rfloor$ and $0 < c < 1$. From Eq. (S12) we obtain simply that

$$\begin{pmatrix} w_1(t_m) \\ w_2(t_m) \\ w_3(t_m) \end{pmatrix} = \begin{pmatrix} u_{11}(t_m) & u_{12}(t_m) \\ u_{21}(t_m) & u_{22}(t_m) \\ u_{31}(t_m) & u_{32}(t_m) \end{pmatrix} \begin{pmatrix} b_1 \\ b_2 \end{pmatrix} \quad \text{(S14)}$$

which is a consistent overdetermined system of equations that can be easily solved.
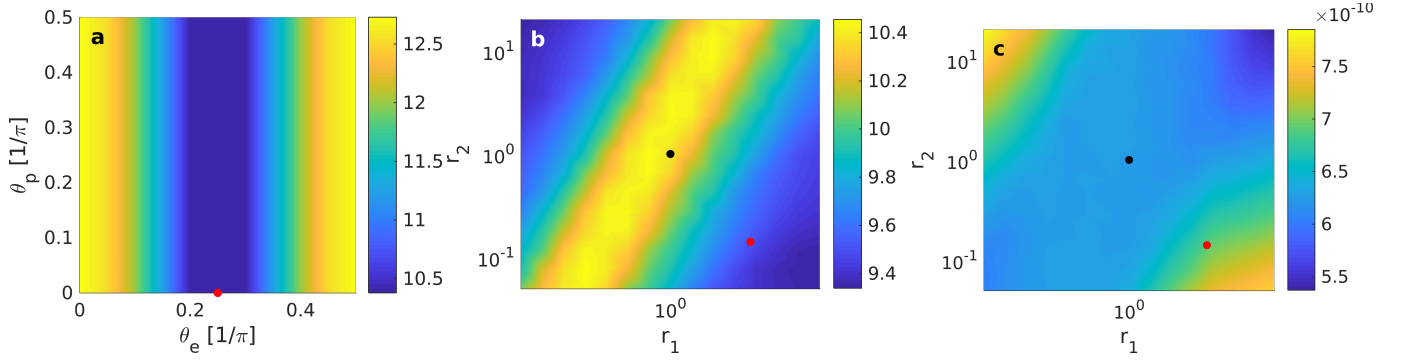
Fig. S1. (**a**) PAPR (dB) of the signal as a function of the relative rotation angle θ_e between the constellations associated to the two different eigenvalues and the relative rotation angle θ_p between the constellations associated to the two different polarizations . The red point marks the values ($\theta_e = \pi/4, \theta_p = 0$) found after the first step of the optimization (PAPR = 10.38 dB). (**b**) PAPR (dB) and (**c**) time-duration (s) of the signal containing 99 % of its power as a function of the radii r_i of the constellations associated to the eigenvalue $\lambda_i, i = 1, 2$. The black point marks the radii used in the first step of the optimization ($r_1 = 1, r_2 = 1$), while the red one marks the optimized values ($r_1 = 5, r_2 = 0.1$) used in the experiment (PAPR = 9.49 dB).

2. CONSTELLATIONS SELECTION

In our work the choice of the constellations of the scattering coefficients $b_{1,2}(\lambda_i)$ was driven by the need to make sure that the time domain signal $E(\tau, \ell)$ has a low peak-to-average power ratio (PAPR), which is defined as

$$\text{PAPR} = 10 \log \left(\frac{\max\left(|E_1|^2 + |E_2|^2\right)}{P} \right) \quad \text{(S15)}$$

where $P = \int_0^T \left(|E_1|^2 + |E_2|^2\right)/T$ is the average power of the field, T its time duration and the index $j = 1, 2$ refers to the two field polarizations. The reason for this is that a signal with high PAPR has lower signal-to-quantization-noise ratio due to the limited resolution of the DAC [?] and is more susceptible to distortion by the devices with a nonlinear characteristic such as Mach-Zehnder modulators (MZMs) and electrical amplifiers [? ?].
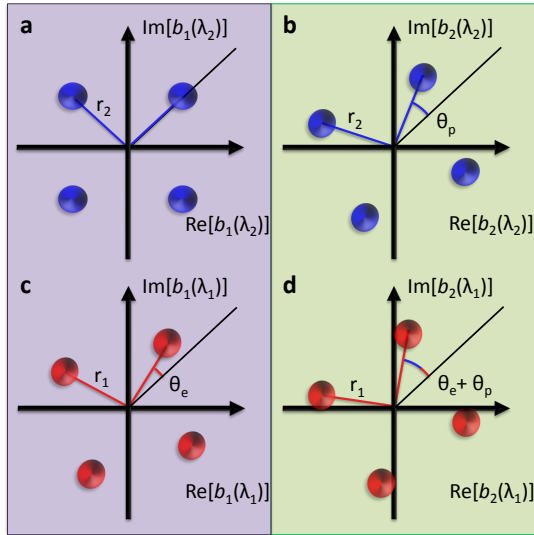

Fig. S2. Representation of the constellations of the scattering coefficients $b_{1,2}(\lambda_i)$, $i = 1, 2$ associated with the eigenvalue $\lambda_1 = i0.3$ (**c,d**) and $\lambda_2 = i0.6$ (**a,b**) and with the first (**a,c**) and second (**b,d**) polarization of the signal. The optimization angles θ_e and θ_p and radii r_1 and r_2 are also shown.

The time domain signal shape, bandwidth, duration and power depend on the particular choice of the eigenvalues and scattering coefficients $(\lambda_1, \lambda_2, b_1(\lambda_1), b_2(\lambda_1), b_1(\lambda_2), b_2(\lambda_2))$. These parameters should be jointly optimized in order to minimize the PAPR while satisfying system specific design constraints. In our case the constraint was to keep the duration of the signal smaller than the time window of 1 ns to avoid cropping the signal. However, this optimization would be computationally demanding given the large dimensionality of the parameters space $\mathbb{C}^6$.

In this work we sacrificed some accuracy in order to simplify the optimization procedure that nonetheless allowed reducing the PAPR of the signal to a level that enabled to transmit over several hundreds of kilometers.

Starting from a reference quadrature phase shift keying (QPSK) constellation $C_r = \exp\left(i\left(k\frac{\pi}{2} + \frac{\pi}{4}\right)\right)$ with $k = 0, 1, 2, 3$ we constructed the set of constellations associated to the scattering coefficient pairs $(b_1(\lambda_i), b_2(\lambda_i))$, $i = 1, 2$ corresponding to the pair of eigenvalues $(\lambda_1 = i0.3, \lambda_2 = i0.6)$ as follow

$$\begin{pmatrix} C_{1,1} & C_{1,2} \\ C_{2,1} & C_{2,2} \end{pmatrix} = \begin{pmatrix} C_r r_1 \exp(i\theta_e) & C_r r_1 \exp(i\theta_e) \exp(i\theta_p) \\ C_r r_2 & C_r r_2 \exp(i\theta_p) \end{pmatrix}$$
(S16)

where $C_{i,j}$ is the constellation associated to the eigenvalue i and polarization j, r_i is the radius of the constellations associated to the eigenvalue λ_i, θ_e is the relative rotation angle between the constellations associated to the two different eigenvalues and θ_p is the relative rotation angle between the constellations associated to the two different polarizations. The four constellation diagrams are represented in Fig. S2.

The PAPR of the signal was optimized in two steps. First the two angles (θ_e, θ_p) were optimized by sweeping their values between 0 and π while having $r_1 = r_2 = 1$. The optimum value of PAPR found is 10.38 dB for ($\theta_e = \pi/4, \theta_p = 0$), which is lower by 2.35 dB compared to the worst case where all four constellations are equal (PAPR = 12.73 dB) as shown in Fig. S1 (a). Note that the optimum value of $\theta_e = \pi/2$ found confirms the results of others previous experimental works in the single polarization case [? ?], while the PAPR seems to be independent on θ_p. To further reduce the PAPR the two radii (r_1, r_2) were then optimized. By varying the radii of the constellations associated to the two eigenvalues it is possible to partially separate the time
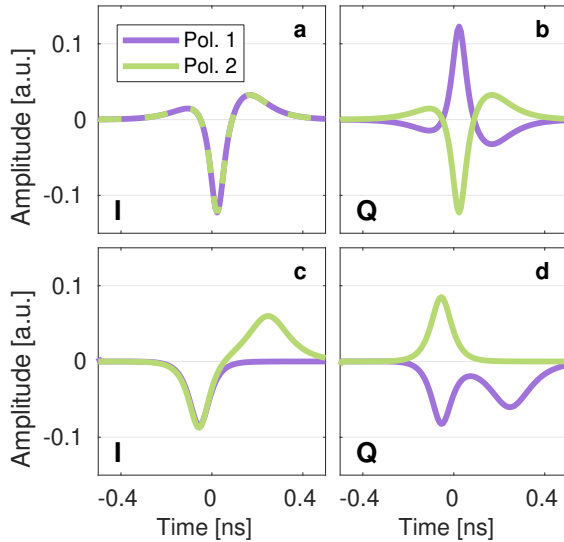
Fig. S3. (**a**) I and (**b**) Q components of one symbol of the signal when all the four constellations are equal to the reference constellation C_r (PAPR = 12.73). (**c**) I and (**d**) Q components corresponding to the constellations used in the experiment (PAPR = 9.49). The violet (Polarization 1) and green (Polarization 2) curves indicates the components associated to the two polarizations.

domain signal components associated to the two eigenvalues. This allows reducing the PAPR at the cost of a longer time duration of the signal as shown in Fig. S1 (b-c). By choosing the set of radii ($r_1 = 5, r_2 = 0.1$) the PAPR results finally in 9.49 dB while the time duration of the signal containing 99 % of its power is still within the time window of 1 ns. In Fig. S3 the in-phase (I) and quadrature (Q) components of one symbol of the time domain signal are shown before and after the optimization of the PAPR.

3. NONLINEAR SPECTRUM NOISE DISTRIBUTION

An analysis of the noise distribution on the eigenvalues and scattering coefficients $b_{1,2}(\lambda_i)$ has been done for the transmission distances of 373.5 km and 332 km performed in the experiment when spans of 41.5 km and 83 km were used respectively. In Fig. S4 the histograms of the received eigenvalues (a,f) and scattering coefficients (b-e, g-l) are shown. The variances of the imaginary part of the received eigenvalues and those of the phase of the scattering coefficients are reported in Table S1.

It is observed that in both cases the variance of the imaginary part of the eigenvalue $\lambda_2 = i0.6$ is about 10% higher than the one of $\lambda_1 = i0.3$. The proportionality of the noise variance on the imaginary part of the eigenvalue is consistent with the predictions made by the model in [?] for the single eigenvalue case.

The variance of the phase of the scattering coefficients $b_1(\lambda_2)$ and $b_2(\lambda_2)$ associated to λ_2 are 2.34 and 2.91 times those of the scattering coefficients $b_1(\lambda_1)$ and $b_2(\lambda_1)$ respectively for the 41.5 km case, and 2.27 and 2.50 for the 83 km case.

Spectral parameter	Noise variance	
	41.5 km case	80.5 km case
$\mathrm{Im}(\lambda_1)$	1.54×10^{-3}	18.06×10^{-3}
$\mathrm{Im}(\lambda_2)$	1.70×10^{-3}	20.39×10^{-3}
$\angle b_1(\lambda_1)$	27.77×10^{-3}	39.00×10^{-3}
$\angle b_2(\lambda_1)$	24.86×10^{-3}	24.62×10^{-3}
$\angle b_1(\lambda_2)$	65.05×10^{-3}	88.40×10^{-3}
$\angle b_2(\lambda_2)$	72.45×10^{-3}	61.52×10^{-3}

Table S1. Variance of the imaginary part of the eigenvalues ($\lambda_1 = i0.3, \lambda_2 = i0.6$) and of the phase of the corresponding scattering coefficients $b(\lambda)$ for the transmission distances of 373.5 km and 332 km when spans of 41.5 km and 83 km are used respectively. Each variance value has been computed over 250000 symbols.
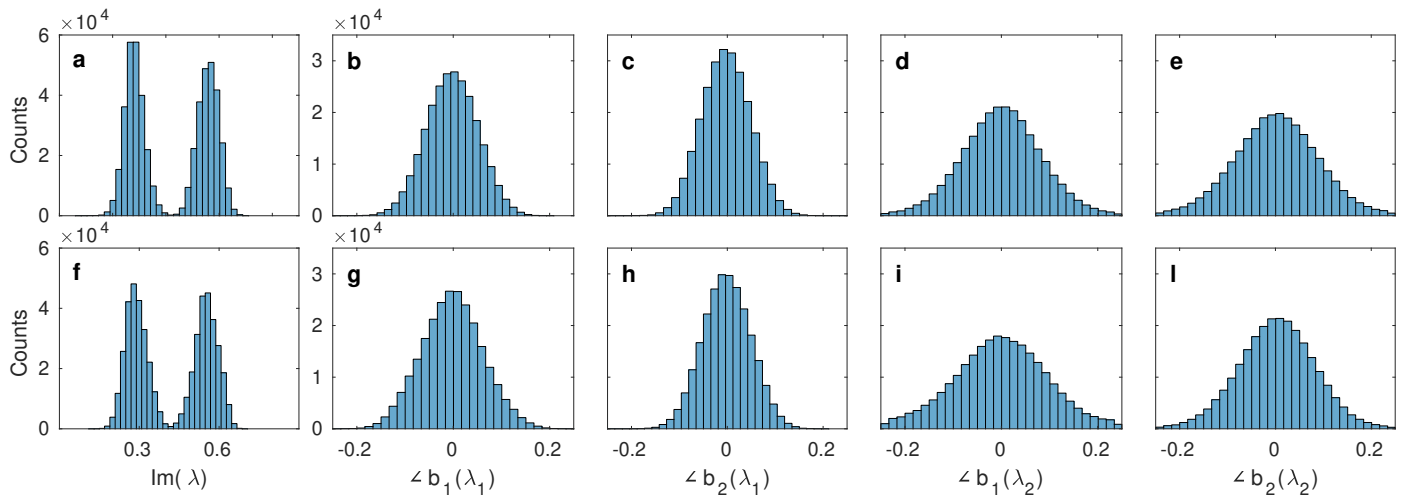
Fig. S4. Distribution of the imaginary part of the received eigenvalues (reference eigenvalues ($\lambda_1 = i0.3, \lambda_2 = i0.6$)) (**a,f**) and phase noise distribution of the scattering coefficients $b(\lambda)$ (**b-e,g-l**) for the transmission distances of 373.5 km and 332 km using spans of 41.5 km (top) and 83 km (bottom) respectively.